Smart Sensors to Reduce Pollutant Emissions in Transportation

Center for Transportation, Environment and Community Health

FINAL REPORT

February 15, 2019

Submitted By:

Ramana Chintalapalle, Mallesham Bandi, Vishal Zade, Aldo Rubio

Center for Advanced Materials Research
The University of Texas at El Paso
500 W. University Ave.
El Paso, TX 79968

DISCLAIMER

The contents of this report reflect the views of the authors, who are responsible for the facts and the accuracy of the information presented herein. This document is disseminated in the interest of information exchange. The report is funded, partially or entirely, by a grant from the U.S. Department of Transportation's University Transportation Centers Program. However, the U.S. Government assumes no liability for the contents or use thereof.

1. Report No.	2. Government Accession No.	3. Recipient's Catalog No.
4. Title and Subtitle Smart Sensors for Integration into Transportation Systems		**5. Report Date** February 15, 2019 **6. Performing Organization Code**
7. Author(s) Ramana Chintalapalle, Mallesham Bandi, Vishal Zade. Aldo Rubio		**8. Performing Organization Report No.**
9. Performing Organization Name and Address Center for Advanced Materials Research University of Texas at El Paso El Paso, TX 79968		**10. Work Unit No.** **11. Contract or Grant No.** 69A3551747119
12. Sponsoring Agency Name and Address U.S. Department of Transportation 1200 New Jersey Avenue, SE Washington, DC 20590		**13. Type of Report and Period Covered** Final Report **14. Sponsoring Agency Code** US-DOT

15. Supplementary Notes

16. Abstract

Doped perovskite materials exhibiting temperature independent conductivity has gained enormous attention for high temperature oxygen sensors due to great advantage over traditional doped metal oxides. This report focused on effect of sintering temperature on structure, morphology to explore correlation between *oxygen sensing response* of $Ba(Fe_{0.7}Ta_{0.3})O_{3-\delta}$ (BFTO30) bulk ceramics with structural and morphological features. Conventional solid-state reaction was used to synthesize BFTO30 powders. Crystal symmetry and phase purity of calcined and sintered powders was confirmed through X-ray diffraction analysis. Calcination of homogenous mixed precursors confirms that a single-phase perovskite phase without any secondary phases was obtained at 1150 °C. Samples were sintered at different temperatures (1200 °C, 1250 °C, 1300 °C, 1350 °C), X-ray diffraction of sintered samples reveals that there is a clear structural transformation from low symmetry rhombohedral phase to high symmetry cubic phase with temperature. Sintered samples exhibit porous morphological features with samples sintered at ≤1300 °C, whereas samples sintered at 1350 °C exhibits dense morphology with nearly spherical grains.

17. Key Words	18. Distribution Statement
Oxygen sensing, Sintering temperature, Solid state reaction	Public Access as well as a resulting journal manuscript submitted, based on which this report is developed.

19. Security Classif. (of this report)	20. Security Classif. (of this page)	21. No of Pages	22. Price
Unclassified	Unclassified	12	

Form DOT F 1700.7 (8-69)

ABSTRACT

Doped perovskite materials exhibiting temperature independent conductivity has gained enormous attention for high temperature oxygen sensors due to great advantage over traditional doped metal oxides. This report focused on effect of sintering temperature on structure, morphology to explore correlation between *oxygen sensing response* of $Ba(Fe_{0.7}Ta_{0.3})O_{3-\delta}$ (BFTO30) bulk ceramics with structural and morphological features. Conventional solid-state reaction was used to synthesize BFTO30 powders. Crystal symmetry and phase purity of calcined and sintered powders was confirmed through X-ray diffraction analysis. Calcination of homogenous mixed precursors confirms that a single-phase perovskite phase without any secondary phases was obtained at 1150 °C. Samples were sintered at different temperatures (1200 °C, 1250 °C, 1300 °C, 1350 °C), X-ray diffraction of sintered samples reveals that there is a clear structural transformation from low symmetry rhombohedral to high symmetry cubic phase with temperature. Sintered samples exhibit porous morphological features with samples sintered at ≤1300 °C, whereas samples sintered at 1350 °C exhibits dense morphology with nearly spherical grains.

Keywords: Oxygen sensing; Sintering temperature; Solid state reaction

ACKNOWLEDGEMENT

This Research is funded by The Center for Transportation, Environment and Community Health (CTECH) awarded by the U.S. Department of Transportation under Contract 69A3551747119.

TABLE OF CONTENTS

LIST OF FIGURES

1. INTRODUCTION

In the past two decades various materials have been studied for O_2 sensor applications to measure and/or monitor the oxygen partial pressure in combustion process of industrial plants and automotive emissions [1, 2]. Oxygen sensors play vital role to improve the performance and fuel efficiency and to minimize the environmental pollution. In order to monitor the exhaust emissions and combustion process the installed oxygen sensor should be long term stable, a quick response to minor variations in oxygen partial pressure and should not show variations in response with temperature gradient [1]. Different types of oxygen sensors such as potentiometric, amperometric and resistive oxygen sensors has been explored. Resistive oxygen sensors have more advantages compared to the potentiometric and amperometric sensors due to independence of reference atmosphere and realization of simple and small structures [1, 2].

In recent years numerous researchers focused on resistive oxygen sensing materials (metal oxides and perovskite oxides) to develop oxygen sensors with high performance. Intrinsic and doped metal oxides based on SnO_2 [3] TiO_2 [3,4], CeO_2 [3, 4] ZrO_2 [3] and Ga_2O_3 [3] has been thoroughly investigated for oxygen sensing applications. Among these SnO_2 is most commercially used material for sensing applications. Semiconducting metal oxides responds to variations in oxygen partial pressure by maintaining the equilibrium between surrounding oxygen and ionic and/or electronic defects present in these oxides. Sensors fabricated using metal oxides has simple design, inexpensive and delivers very good sensing performance. However, a major drawback of most of the metal oxides is significant interference of temperature while operating in extreme conditions [3]. Therefore, in the way of finding new materials for oxygen sensor applications, perovskite oxides such as doped Sr, Ba and Ca based materials ($SrTiO_3$, $BaTiO_3$ and $CaTiO_3$) has been studied both in the form of bulk and thin films [1, 3, 5].

Due to high melting point and decomposition temperature perovskite oxides are particularly attractive for high-temperature applications. High melting point and decomposition temperature of these materials provide microstructural and morphological stability to improve reliability and long-term sensor performance. Moreover, the perovskite oxides have two differently-sized cations at A and B site, these two cation sites allow doping the different elements. Flexibility of doping different elements allows to control the transport and catalytic properties, as consequence sensor performance is optimized for particular sensing application. Among these perovskite oxides Fe doped $SrTO_3$ is suggested as temperature independent oxygen sensing material by William et al [3].

However, the temperature independency is ruled out by Rothschild et al., due to decomposition into strontium titanite and strontium ferrite at exhaust conditions [3]. Recently $Ba(Fe_{1-x}Ta_x)O_{3-\delta}$ (BFTO) reported as temperature independent oxygen sensor material over 400-900 ˚C temperature range. To the best of our knowledge there is no much literature of BFTO compounds. Hence, the present project mainly focused in understanding the BFTO compounds both in ***bulk and thin film***

form. Moreover, from the literature it is found that $Ba(Fe_{0.7}Ta_{0.3})O_{3-\delta}$ shows highest oxygen sensing response up to 900 °C. Hence, the objective of this research focused on the effect of sintering temperature on oxygen sensing response of $Ba(Fe_{0.7}Ta_{0.3})O_{3-\delta}$ bulk ceramics. In this report, the progress achieved in understanding the structural and morphological properties of bulk ceramics has been discussed.

2. EXPERIMENTAL DETAILS

2.1. Synthesis

Conventional solid state reaction route was used to synthesize $Ba(Fe_{0.7}Ta_{0.3})O_{3-\delta}$ [BFTO30] ceramic powder using commercially available precursors. To synthesize BFTO30 powder high purity precursor materials such $BaCO_3$ (99.9%, Sigma Aldrich), Fe_2O_3 (99.9%, Sigma Aldrich) and Ta_2O_5 (99.9%, Sigma Aldrich) were weighed stoichiometric proportion accordance with respective composition. Stoichiometrically weighed precursors homogeneously grounded in an agate mortar using acetone as wetting media.

Homogeneously grounded powders were calcined at different temperatures (1000 °C, 1050 °C, 1100 °C and 1150 °C) to achieve phase purity Calcined powders were grounded again, pellets of 8mm diameter and 1 mm thick samples were prepared using a die and uniaxial hydraulic press by applying load of 1.5 ton. In order alter the porosity and morphological features, the obtained pellets were sintered in Muffle furnace at different temperatures (1200°C, 1250 °C, 1300 °C and 1350 °C). The sintered ceramic samples were analyzed using X-ray diffraction, Scanning Electron Microscopy to understand quality of structural, morphological features.

2.2. Characterization

X-ray diffraction (XRD): X-ray diffraction is a versatile known technique to determine crystal symmetry and phases present in a given compound. In the present work, Rigaku X-ray diffractometer [Mini Flex II] was used to analyze calcined and sintered samples at room temperature). Scanning parameters were: 10° – 80°(2θ range), step size – 0.02° and Scan rate – 0.6°/min. *Scanning Electron Microscope [SEM]:* The microstructural features of sintered samples were analyzed using SEM. Samples were coated with silver using sputter coater prior to imaging to avoid commonly encountered charging effect in SEM while imaging insulating samples.

3. RESULTS AND DISCUSSIONS

3.1. Structural Analysis

Figure 1 shows the X-ray diffraction patterns of $Ba(Fe_{0.7}Ta_{0.3})O_{3-\delta}$ calcined at different temperatures. X-ray diffraction patterns of calcined samples clearly reveals that at low calcination temperature unreacted Ta_2O_5 found as secondary phase along with perovskite phase. Asterisk (*) in the figure shows the Ta_2O_5 secondary phase. The single perovskite phase formation without any secondary phases was noticed at sample calcined at 1150 °C. In present study we calcined samples at different temperatures (1000 °C, 1050 °C, 1100 °C) by intermediate grinding which will helpful to complete the reaction and stabilize the structure. The formation of secondary phase at lower calcination temperatures might be attributed to BFTO30 ceramics may require high calcination temperature when they synthesized through conventional solid-state reaction route.

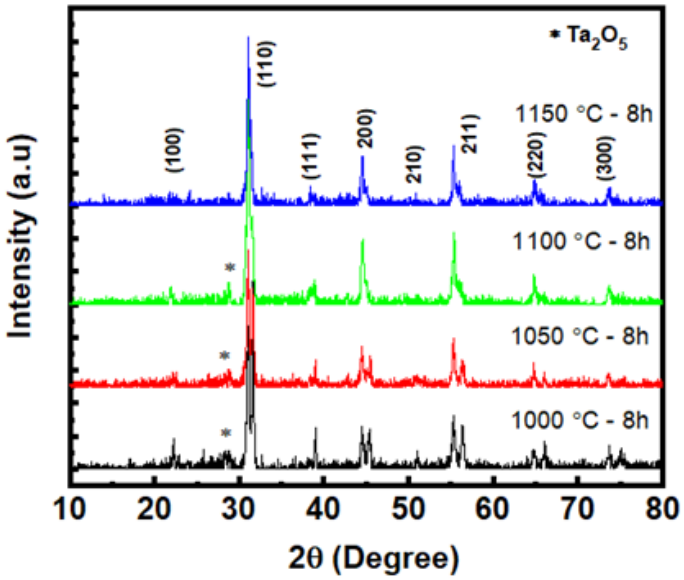

Figure 1 – X-ray diffraction pattern of Ba

Figure 2 shows X-ray diffraction pattern of Ba $(Fe_{0.7}Ta_{0.3})O_{3-\delta}$ samples sintered at different temperatures. Diffraction patterns clearly reveals all the samples are stabilized in perovskite structure without any secondary phase. Interestingly we have observed structural phase transformation with increasing sintering temperatures. Samples sintered at 1300 °C and 1350 °C exhibits pseudo cubic perovskite structure, whereas samples sintered at 1200 °C and 1250 °C exhibits low symmetry phase. However, stability and symmetry of perovskite structure was determined by Goldschmidt tolerance factor (t) based on the chemical formula given by [1]:

$$t = \frac{R_A + R_O}{\sqrt{2}\,(R_B + R_O)} \quad (1)$$

Where, R_A and R_B are the ionic radii of A site and B site cations, R_O is ionic radius of oxygen. The Shannon ionic radii [1] of constituent elements include: 1.61 Å (Ba^{2+}), 0.64 (Ta^{5+}), 0.645 (Fe^{3+}, high spin state), 0.55 (Fe^{3+}, low spin state) and 1.4 (O^{2-}). The estimated tolerance factor values with Fe^{3+} high spin and low spin states are 1.07 and 1.11 respectively. Tolerance factors values (>1) reveals that the compound should be stabilized in hexagonal or tetragonal phase due to higher difference between A site and B-site ionic radii. In contradiction to tolerance factor values, difference in splitting behavior of Bragg planes with increasing temperature clearly reveals that a clear structural transformation with increasing sintering temperature. The splitting in (200) reflection is a characteristic behavior of tetragonal phase. Figure 3 high resolution patterns of (200) reflection, representing a pronounced splitting at lower sintering temperatures (1200 °C and 1250 °C), whereas at 1350 °C does not show noticeable splitting.

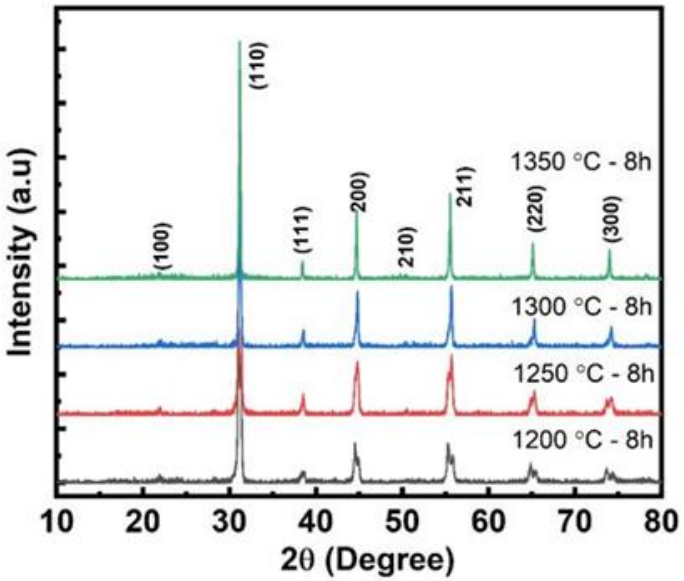

Figure 2 – X-ray diffraction patterns of Ba ($Fe_{0.7}Ta_{0.3}$) $O_{3-\delta}$ sintered at different temperatures

All the reflections of samples sintered at 1350 °C is singlet with asymmetry at lower Bragg angle, such as asymmetry in Bragg reflections might be attributed to pseudo cubic phase. But at lower sintering temperatures along with (200) reflections (211) and (220) peaks exhibiting doublet feature. Hence, such splitting features rules out the attributing the tetragonal phase to samples sintered at lower temperatures. Doublet features of (211) and (220) might be attributed at lower sintering temperature attributed to rhombohedral phase. Figure 4 represents the high-resolution

pattern of (211) reflection with Gaussian curve fitting. However, extensive analysis of samples to determine the exact crystal symmetry through structural refinement using Rietveld method and Selected area electron diffraction (Transmission Electron Microscopy).

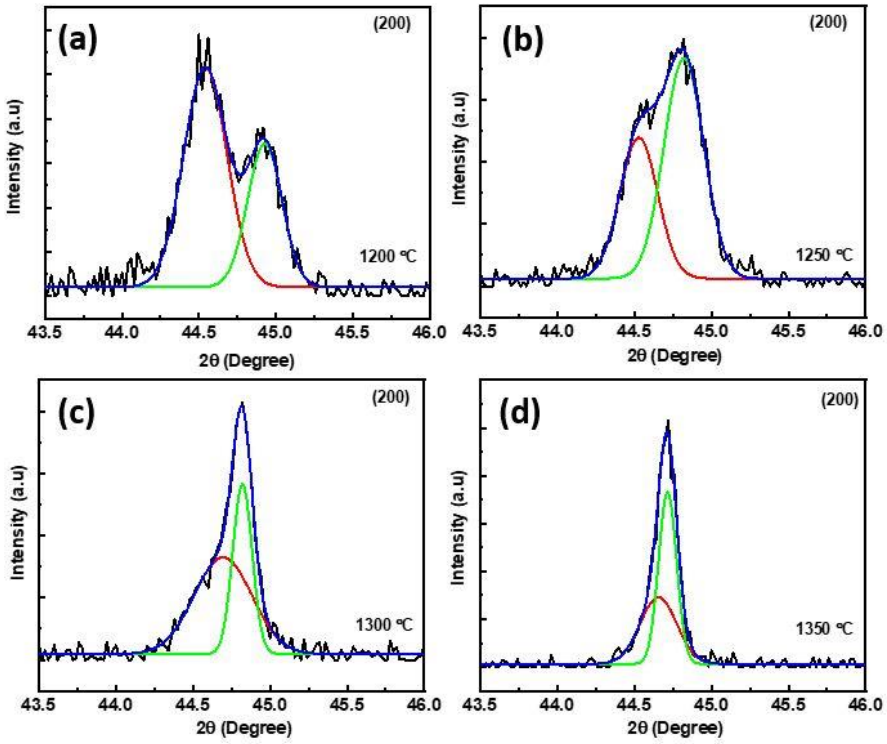

Figure 3 – Gaussian fitting of high-resolution pattern of (200) reflection (a characteristic peak of tetragonal phase)

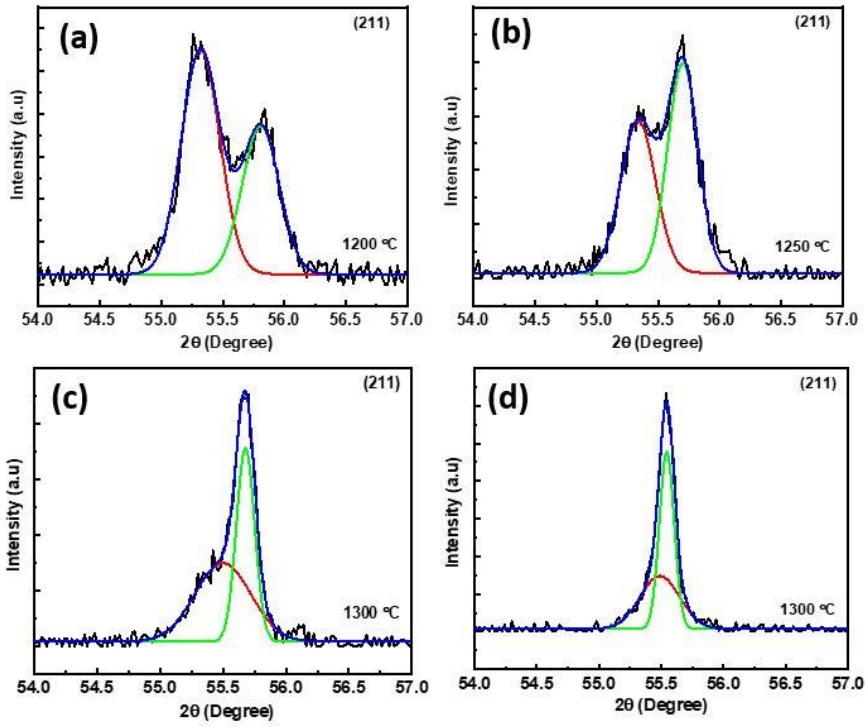

Figure 4 – Gaussian fitting of high-resolution pattern of (211) reflection

3.2. Morphological Studies

It is known that along with crystal structure and electronic structure, surface morphology will also play key role in gas sensing behavior of semiconductor oxides. Hence, it very important to know surface morphology of these ceramics to explore the best sintering temperature and optimized sensing behavior. Figure 5. shows the Scanning Electron Microscope (SEM) images of samples sintered at different temperatures. Samples sintered at 1200 °C, 1250 °C and 1300 °C exhibits porous structure varying porosity percentage, whereas samples sintered at 1350 °C exhibits close packed grains with nearly spherical shape. We also estimated the porosity of these samples using ***ImageJ***; the estimated porosity of these samples includes: ≈ 14%, ≈ 4%, ≈ 7% and ≈ 1% respectively with increasing sintering temperature.

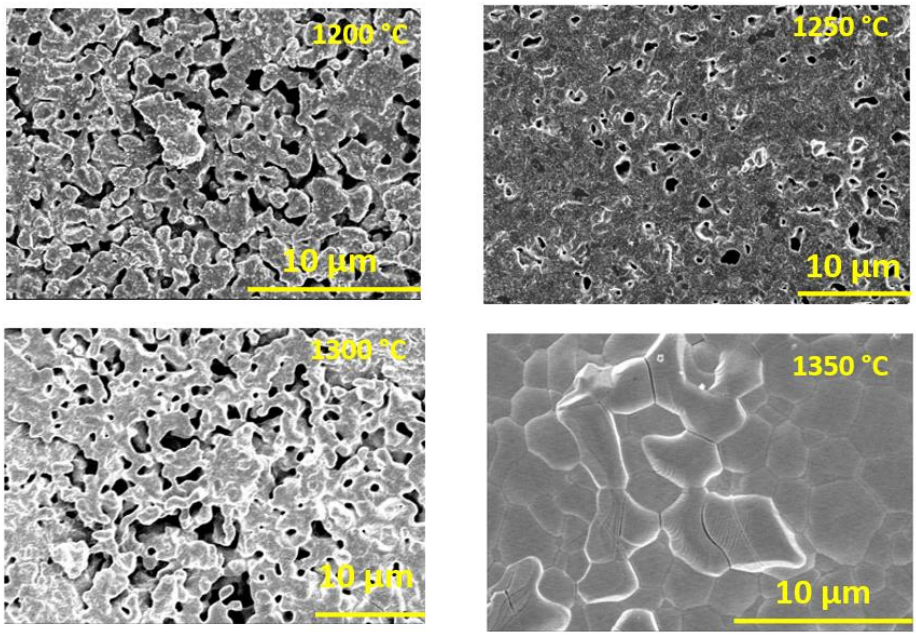

Figure 5 – SEM images of Ba ($Fe_{0.7}Ta_{0.3}$) $O_{3-\delta}$ sintered at different temperatures

4. FUTURE WORK

Based on the results discussed, we proposed the following two items as directions for future research:

1. Measuring the ***oxygen sensing response*** of bulk ceramic pellets sintered at different temperatures and understanding the correlation between sensing response and aforementioned structural and morphological properties.

2. Fabrication of ***polycrystalline thin films and nanostructures*** of $Ba(Fe_{1-x}Ta_x)O_{3-\delta}$ using pulsed laser ablation (PLD) technique in order to tune the oxygen response times.

REFERENCES

[1]. J. W. Fergus, Perovskites for semiconductor-based gas sensors, Sensors and Actuators B 123 (2007) 1169–1179.

[2]. C. Y. Chen and K. H. Chang, Temperature independent resistive oxygen sensor prepared using

[3]. zirconia-doped ceria powders, Sensors and Actuators B: Chemical 162 (2012) 68-75.

[4]. M. Bektas, D. Schonauer-Kamin, G. Hagen, A. Mergner, C. Bojer, S. Lippert, W. Milius, J. Breu, R. Moos, BaFe1-xTaxO3-δ A material for temperature independent resistive oxygen sensors, Sensors and Actuators B 190 (2014) 208– 213.

[5]. C. Argirusis, F. Jomard, S. F. Wagner, W. Menesklou, E. Ivers-Tiffée, Study of the oxygen incorporation and diffusion in Sr(Ti0.65Fe0.35)O3 ceramics, Solid State Ionics 192 (2011) 9–11.

FURTHER READINGS

[1]. A. Rothschild, Scott J. Litzelman H.L. Tuller, E. Ivers-Tiffee, W. Menesklou, T. Schneider and E. Ivers-Tiffee, Temperature-independent resistive oxygen sensors based on SrTi1−xFexO3−δ solid solutions, Sensors and Actuators B 108 (2005) 223–230.

[2]. M.C. Carotta, A. Cervi, S. Gherardi, V. Guidi, C. Malagu, G. Martinelli, B. Vendemiati, M. Sacerdoti, G. Ghiotti, S. Morandi, S. Lettieri, P. Maddalena, A. Setaro, (Ti, Sn)O2 solid solutions for gas sensing: A systematic approach by different techniques for different calcination temperature and molar composition, Sensors and Actuators B 139 (2009) 329–339.

[3]. A. Takami, Development of titania heated exhaust gas oxygen sensor, Ceram. Bull. 67 (1988) 1956–1960.

[4]. E.M. Logothetis, W.J. Kaiser, TiO2 film oxygen sensors made by chemical vapor deposition from organometallics, Sensor. Actuat. 4 (1983) 333–340.

[5]. N. Izu, W. Shin, I. Matsubara, N. Murayama, Development of resistive oxygen sensors based on cerium oxide thick film, J. Electroceram. 13 (2004) 703–706.

[6]. N. Izu, W. Shin, I. Matsubara, N. Murayama, Development of resistive oxygen sensors based on cerium oxide thick film, J. Electroceram. 13 (2004) 703–706.

[7]. J. Riegel, H.-M. Wiedenmann, H. Neumann, Exhaust gas sensors for automotive emission control, Solid State Ionics 152–153 (2002) 783.

[8]. U. Hoefer, J. Frank and M. Fleischier, High temperature Ga2O3 gas sensors and SnO2 gas sensors: a comparison, Sensors and Actutors B 78 (2001) 6-11.

[9]. K. Sahner, R. Moos, N. Izu, W. Shin and N. Murayama, Sensors and Actutors B 113

[10]. H. Y. Li, H. Yang and X. Guo, Oxygen sensors based on SrTi0.65Fe0.35O3-δthick film with MgO diffusion barrier for automotive emission control, Sensors and Actuators B 213 (2015) 102–110.

[11]. D.E. Williams, P. McGeehin, B.C. Tofield, Oxygen Sensors, US Patent 4,54,494 (1982).

[12]. A. Rothschild, W. Menesklou, H.L. Tuller, E. Ivers-Tiffee, Electronic Structure, Defect Chemistry, and Transport Properties of SrTi1-xFexO3-y Solid Solutions, Chem. Mater. 18 (2006) 3651–3659.

[13]. W. C. Lee, C. Y. Huang, L. K. Tsao, Y. C. Wu, Chemical composition and tolerance factor at the morphotropic phase boundary in (Bi0.5Na0.5)TiO3 based piezoelectric ceramics, Journal of the European Ceramic Society 29 (2009) 1443–1448.

[14]. R. D. Shannon, Revised effective ionic radii and systematic studies of interatomic distances in halides and chalcogenides. Acta Crystallogr., Sect. A, 32 (1976) 751-767.